

# Predicting compressive strength of CRM samples using Image processing and ANN

M I Waris<sup>1</sup>, J Mir<sup>2</sup>, V Plevris<sup>3</sup> and A Ahmad<sup>1,4</sup>

<sup>1</sup> Department of Civil Engineering, University of Engineering and Technology Taxila, Punjab, Pakistan

<sup>2</sup> Department of Electrical Engineering, University of Engineering and Technology Taxila, Punjab, Pakistan

<sup>3</sup> Department of Civil Engineering and Energy Technology, OsloMet- Oslo Metropolitan University, Oslo, Norway

<sup>4</sup> Corresponding author E-mail: afaq.ahmad@uettaxila.edu.pk

**Abstract.** Quality of concrete is majorly ascertained through its compressive strength which has a significant role in the stability of concrete structures. In this study, artificial neural network (ANN) and image processing (IP) techniques were used to predict the concrete compressive strength ( $f_c$ ) with cement replacement material (CRM), i.e., Fly Ash (FA) and Silica Fumes (SF). 18 concrete cylinders were cast with different mix ratios and with different % of CRM. Half of them were tested for compression strength in the laboratory and remaining cylinders were cut into three slices each, for prediction of compressive strength through the proposed technique. Images were obtained using a DSLR camera under defined conditions to extract the features. Based on the extracted features, ANN modelling was performed for predicting  $f_c$ . A comparison of experimental results and ANN results ( $R = 0.9865$ ) proved ANN models can be used as a prediction tool for compressive strength of concrete.

**Keywords**—Artificial neural network, image processing, concrete, compressive strength,

## 1. INTRODUCTION

Machines are employed to devise algorithms from the acquired data to predict desired outcomes. Artificial neural networks (ANN) and image processing (IP) are popular techniques in artificial intelligence utilized to solve complex and time-consuming problems in the field of engineering and science. ANN is a computational network consisting of different interconnecting layers and neurons used to perform the duties of a biological mind. IP is the process of extracting useful information from images with the aid of a computer algorithm. From the past few decades, researchers have been using ANN and IP in the field of civil engineering to study building materials, concrete technology, structural engineering, and morphology of building materials [1-9]. Amongst the building materials, concrete: a composite material made up of cement, sand, and aggregate bonded together [1, 10], has a major role in the stability of structures. Concrete exhibits heterogeneous structure with a non-linear behavior and is extensively used in buildings, bridges, dams, and roads because of its nature of high compressive resistance. The main characteristic of concrete is the compressive strength  $f_c$ , which has a direct impact on other characteristics that can be measured from the concrete compressive strength [11].

Based on the application, the compressive strength  $f_c$  of concrete can be studied through various conventional test methods, such as Schmidt hammer, ultrasonic pulse velocity, core drilling, electrical resistivity measurement, etc. These methods can be mainly categorized into two approaches: destructive and non-destructive testing [5, 12]. Though efficient, these methods demand specialized equipment for making concrete compressive strength measurements and are, therefore, labor-intensive, expensive and time-consuming. To address these shortcomings, a new non-destructive technique is recently proposed



in [11] as an alternative to traditional concrete compressive strength measuring methods. The method estimates the compressive strength of concrete with an accuracy of 99.8% using ANN and IP. However, the effectiveness and validation of this vision-based approach is not investigated when cement replacement material is utilized partially in the concrete.

In this paper, a computer-vision based approach employing ANN and IP is presented to predict the compressive strength  $f_c$  of the concrete. For this, 18 cylindrical samples with different mix design ratios and cement replacement material percentages were cast and cured. Then, concrete surface images were acquired from which statistical features such as mean, median and standard deviation were extracted using IP. These features were utilized for training the ANN architecture to predict the compressive strength which is then compared with the actual measurements for validation.

The rest of the paper is organized as follows. Section 2 provides the specimen preparation and testing details. Section 3 discusses the IP algorithms and ANN architecture, utilized for image acquisition, feature extraction, and training. Finally, Section 4 concludes the paper with results and discussions.

## 2. SPECIMEN PREPARATION AND TESTING

### 2.1. Materials and Mixing

For casting the concrete samples, ordinary portland cement (OPC) as per the specification of ASTM C150 Type I with aggregate and river sand (locally available in Pakistan) were used. Cement replacement materials (CRM) such as Silica fume ( $SF$ ) and fly ash ( $FA$ ) were utilized to replace cement by volume in the mixture by 0%, 15%, 25%. The chemical compositions of OPC,  $SF$  and  $FA$  are given Table 1. Selected mix proportions to prepare different concrete mixes are tabulated in Table 2. Mixtures were prepared under the natural environment. Then, 18 concrete cylindrical specimens of dimension 150 mm  $\times$  300 mm were cast and cured in the natural water for 14 days. The concrete samples were left in the air to dry for 24 hours before performing compressive strength tests.

**Table 1.** Chemical composition of cement, silica fume and fly ash.

	Cement	$SF$	$FA$
Silica	22.5	84 – 86	57 – 65
Aluminum oxide	5.0	1.0 (max.)	28 – 32
Iron oxide	4.0	2.0 – 3.5	1 – 4
Calcium oxide	64.25	1.0 – 1.5	1 – 2
Loss on ignition	0.64	4 – 7	9.01

**Table 2.** Samples mix ratio with CRM by percentage of volume of cement.

Sample	Mix Ratio	W/C Ratio	% $FA$	% $SF$	14 Days Curing
7S0.4W0A	1:2:4	0.4	0	0	2
7S0.5W0A	1:2:4	0.5	0	0	2
7S0.6W0A	1:2:4	0.6	0	0	2
7S0.4W15A	1:2:4	0.4	15	15	2
7S0.5W15A	1:2:4	0.5	15	15	2
7S0.6W15A	1:2:4	0.6	15	15	2
7S0.4W25A	1:2:4	0.4	25	25	2
7S0.5W25A	1:2:4	0.5	25	25	2
7S0.6W25A	1:2:4	0.6	25	25	2

### 2.2. Compressive Strength $f_c$

The casted cylindrical concrete samples containing cement replacement material  $FA$  and  $SF$  with 0%, 15%, 25% by weight of cement were tested to obtain the compressive strength  $f_c$ . The  $f_c$  was measured according to ASTM 39 on a cylindrical specimen of dimension 150 mm  $\times$  300 mm for each mix ratio cured at 14 days.

## 3. IMAGE PROCESSING AND ARTIFICIAL NEURAL NETWORK

### 3.1. Image acquisition setup

As the efficiency of any image processing based technique largely depends upon the quality of the images, special arrangements were made to ensure that the acquired images of the prepared cylindrical specimens were free of any noise, light variation or shadows. For this, the imaging lab was built in a small room of dimension 3 m  $\times$  3 m. First, the sunlight was blocked by using black sheets on each entry point of light. Then, two 30W LED bulbs were used to produce artificial light of 2000 lux to illuminate the specimens [11] for image acquisition. This ensured the uniform illumination in the room which allowed to capture images without generating any unwanted shadows.

### 3.2. Cutting of concrete samples

Nine of the 18 concrete cylinder samples were cut horizontally using sawing machine into three slices with each slice having the same size (150 mm diameter and 101.6 mm height). Top and bottom faces of the cylinder slices were labelled, as depicted in Fig.1.

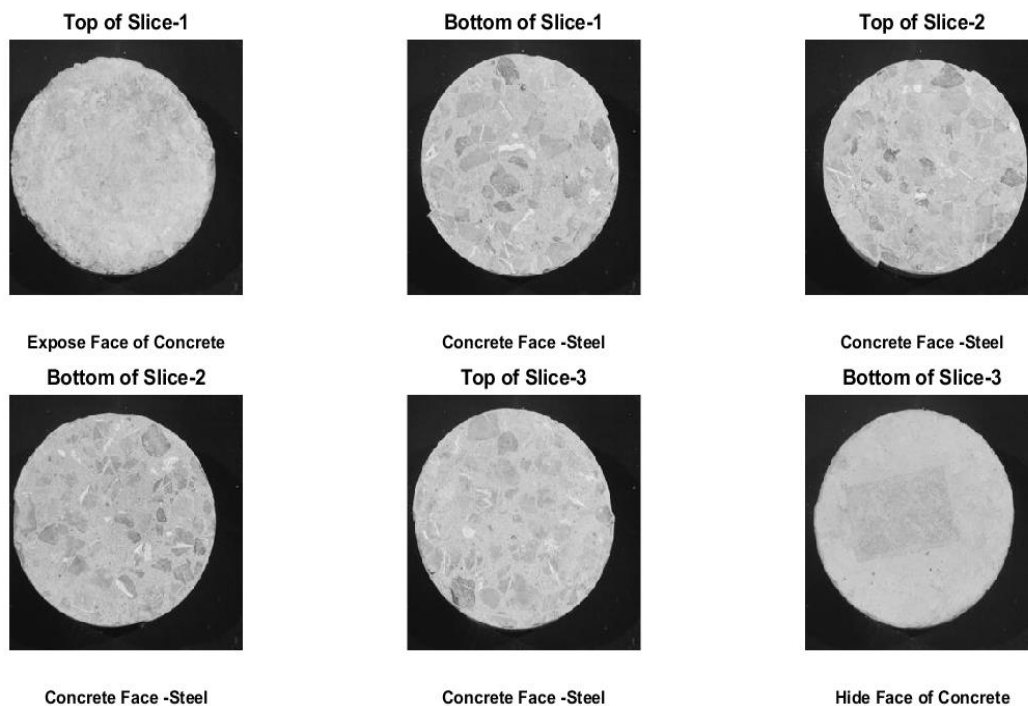


**Figure 1.** Top and bottom faces of three slices of concrete cylinder.

### 3.3. Image acquisition and Feature Extraction

Pictures of the slice surfaces of the specimen were acquired with DSLR NIKON 3300 camera mounted 300 mm vertically above the sample surface. The camera had a 24-million-pixel capacity. Accounting the top and bottom faces of three slices, six colored images in total were taken for each concrete cylindrical specimen. The captured images are digital where each value, generally referred to as a pixel, represents the brightness of the image at that point. Then, the images were converted into the grayscale representation  $I$  using (1), where  $R$ ,  $G$  and  $B$  represents the red, green and blue colour pixel values, respectively.

$$I = 0.2290 \times R + 0.558 \times G + 0.113 \times B \quad (1)$$

After the grayscale conversion, the images are resized to  $256 \times 256$  resolution for further processing. To ensure the structural details are not changed due to down-sampling, the image is low pass filtered before the application of resizing. Once the images are resized, statistical features like mean  $\bar{I}$ , median  $\tilde{I}$ , and standard deviation  $\sigma_I^2$  are to be calculated using (2), (3) and (4), respectively [10], where  $n$  is the total number of pixel values in grayscale image  $I$ .

$$\bar{I} = \frac{1}{n} \sum_{i=1}^n I \quad (2)$$

$$\tilde{I} = \{(n + 1) \div 2\}^{Th} \quad (3)$$

$$\sigma_I^2 = \sqrt{\frac{1}{n} \sum_{i=1}^n (I - \bar{I})^2} \quad (4)$$

The statistical features are to be extracted from region of interest only, i.e., the concrete surface in the image and not from the background portion of the image. To ensure this, the masks are generated as shown in Fig. 3 using thresholding technique by extracting the threshold value from the histograms depicted in Fig. 2.

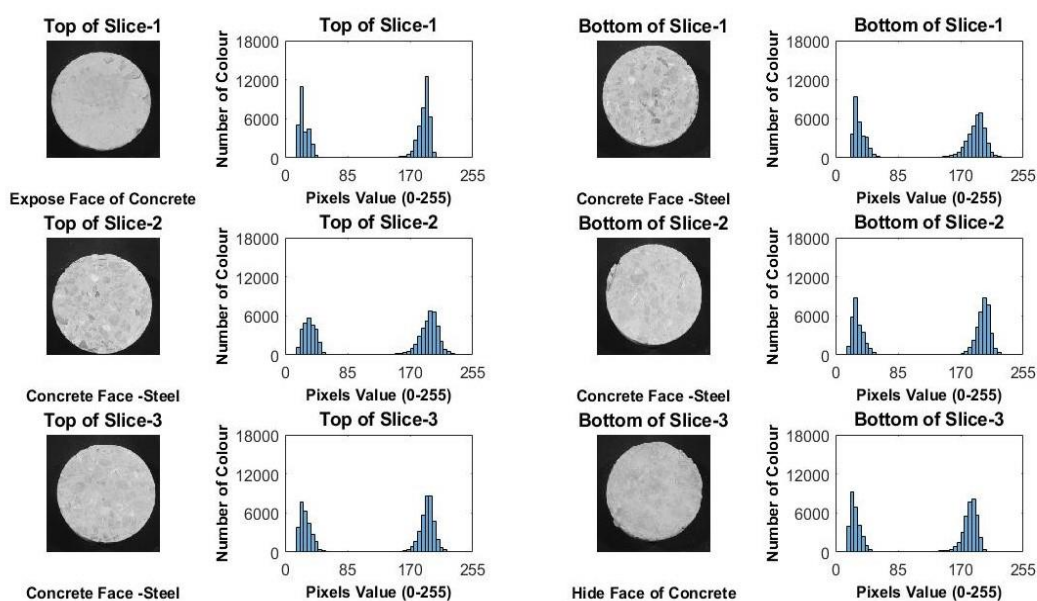


**Figure 2.** Histogram of pixel values of six faces of concrete cylinder slices.

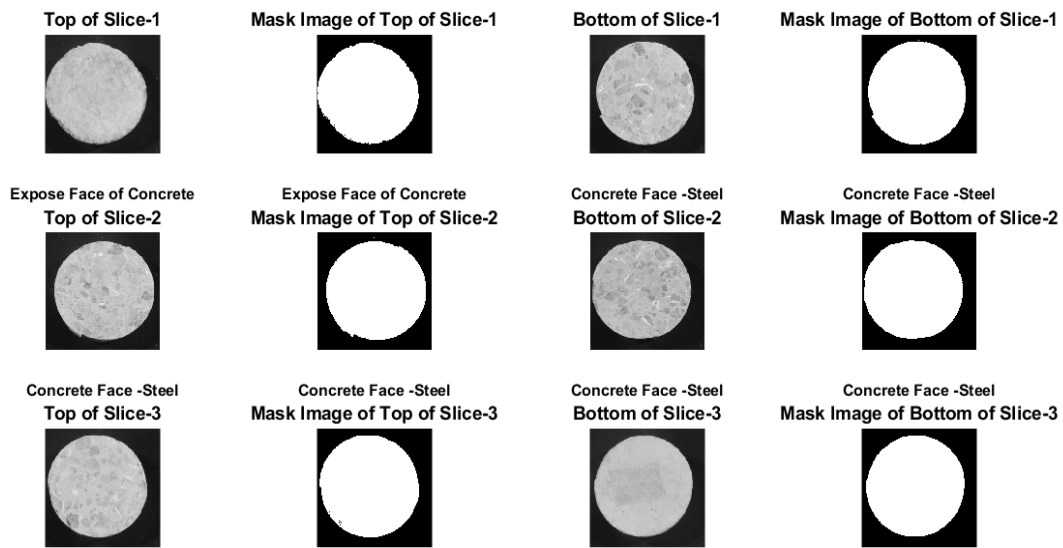


**Figure 3.** Masking of top and bottom faces of three slices of concrete cylinder.

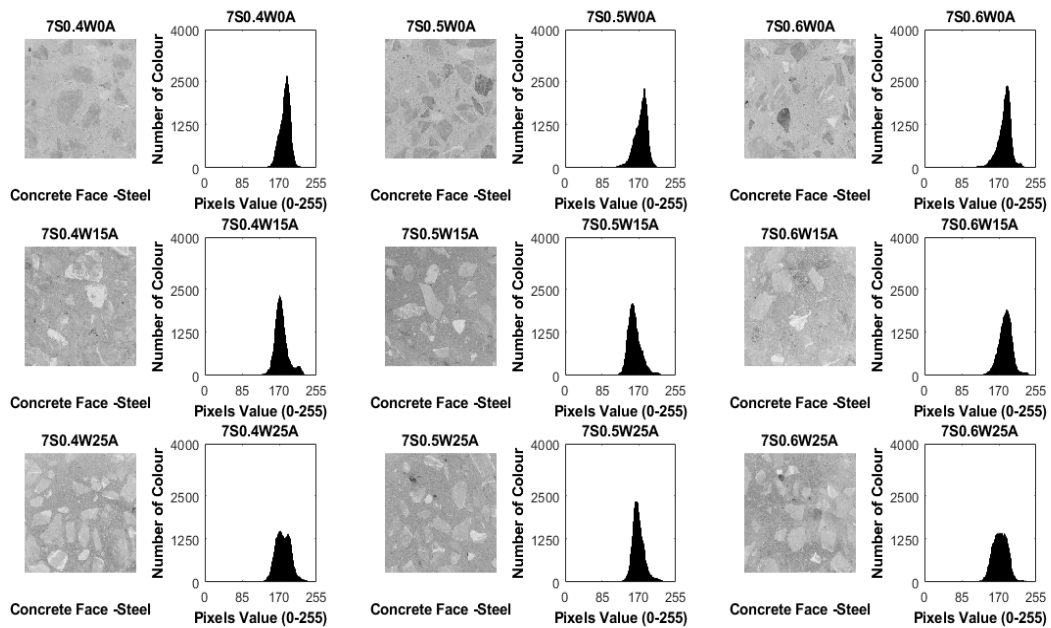


**Figure 4.** Histogram of center faces of concrete specimen of all mix ratios.

The effect of *SF*, *FA* and water cement ratio (*W/C*) on air voids can be observed in Fig. 4, which shows the top concrete image of the centre slice for all mix ratios after the application of masking. Clearly, the distribution of histograms is different for different mix ratios from which it can be inferred that statistical features will characterize the image representation and thereby its properties like compressive strength.

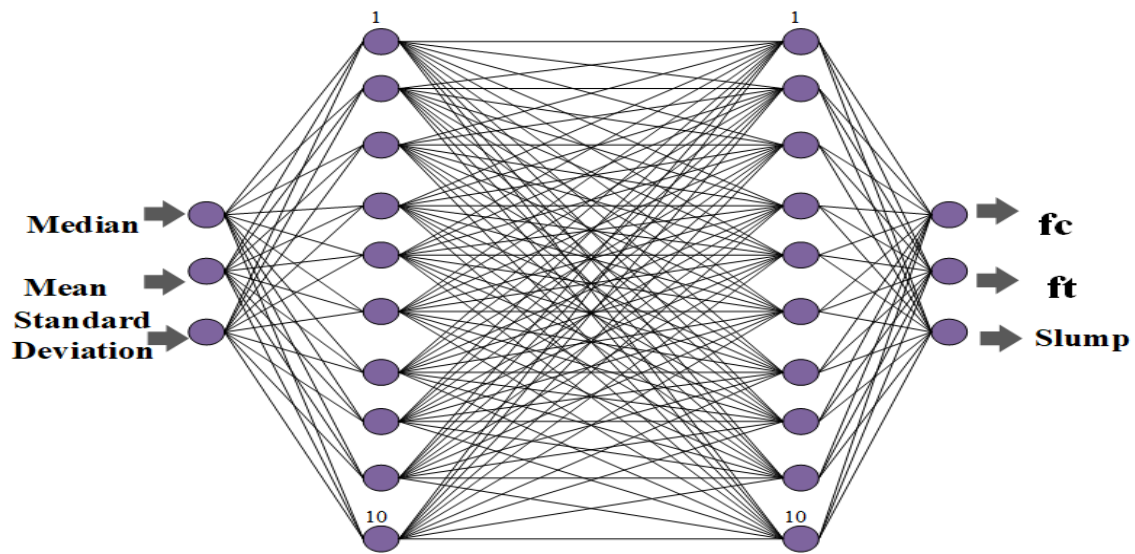


**Figure 5.** Architecture of the optimized ANN model.

### 3.4. ANN architecture and Training

ANN is a set of layers and nodes used to process information similar to the human brain. In our method, the Levenberg-Marquardt (LM) back-propagation ANN model was adopted to process the data. The extracted statistical features of standard deviation, mean and median were taken as input and experimental values of compressive strength, tensile strength, and slump obtained from laboratory tests were used as target values. Before training, normalization of input and output values between 0 and 1 was done using (5), where  $Z_s$  represents normalized value of the variable  $u$  and  $u_{min}$  and  $u_{max}$  are the minimum and maximum values of the variable  $u$ , respectively.

$$Z_s = \frac{(u - u_{min})}{(u_{max} - u_{min})} \quad (5)$$

The optimum model was found after many trails and adjusting learning values and moment constant [11]. The architecture of the optimized ANN model with one input layer, two hidden layers with ten neurons each and one output layer for this study, is shown in Fig. 5. After developing the initial ANN architecture, the training process was repeated iteratively to obtain an optimum ANN model. An optimized model was obtained with 10000 iteration number which was tested against various tuning parameter values during the process. The model that gives the highest accuracy was selected. The selected iteration value is the ideal iteration number related to the sampled problem. So, the best ANN model was found for the minimum training and testing error. The formula for the training and testing errors is given in (6)

$$ET(\%) = \left( \sum_{n=1}^k \frac{|a(n) - b(n)|}{m * j} \right) * 100 \quad (6)$$

Here,  $a(n)$  represents the desired output values,  $b(n)$  represents the ANN outputs,  $k$  represents the number of data points in the training and testing data,  $m$  represents segment numbers in the training and testing data, and  $j$  represents the ANN outputs for the training and testing operations.

#### 4. RESULTS AND DISCUSSIONS

In the presented work, a combination of two artificial techniques IP and ANN was applied to determine the compressive strength of concrete, which is the significant construction material in civil engineering. Experimental results and the results from the adopted method were compared and found similar. The accuracy of the results obtained by our technique is 98.65%. Following are few key observations.

- Numerous factors affect the mechanical properties of concrete. A data set could be produced including all such parameters water/cement ratio, curing, additives, the quantity of cement, compaction, size of aggregate, size and shape of the specimen.
- In this study, the ANN model with two hidden layers and 10 nodes was selected, other effective parameters  $l_r$  and  $m_c$  were 0.9 and 0.2, respectively. Chosen parameters affect the performance of ANN such as processing time, accuracy, etc.
- In the present study, different parameters are chosen for concrete are for a different purpose. Different combinations of parameters are used mainly because of their effect on the mechanical properties of concrete. Therefore, results are specific to the parameters used which is a limitation of the current study.

#### 5. REFERENCES

- [1] A. J. Tenza-Abril, Y. Villacampa, A. M. Solak, and F. Baeza-Brotons, "Prediction and sensitivity analysis of compressive strength in segregated lightweight concrete based on artificial neural network using ultrasonic pulse velocity," *Construction and Building Materials*, vol. 189, pp. 1173-1183, 2018.
- [2] C.-Y. Kao, C.-H. Shen, J.-C. Jan, and S.-L. Hung, "A Computer-Aided Approach to Pozzolan Concrete Mix Design," *Advances in Civil Engineering*, vol. 2018, pp. 1-15, 2018.
- [3] T. Gupta, K. A. Patel, S. Siddique, R. K. Sharma, and S. Chaudhary, "Prediction of mechanical properties of rubberised concrete exposed to elevated temperature using ANN," *Measurement*, vol. 147, 2019.
- [4] P. Chopra, R. K. Sharma, and M. Kumar, "Prediction of Compressive Strength of Concrete Using Artificial Neural Network and Genetic Programming %J Advances in Materials Science and Engineering," vol. 2016, p. 10, 2016, Art. no. 7648467.
- [5] J. A. Bogas, M. G. Gomes, and A. Gomes, "Compressive strength evaluation of structural lightweight concrete by non-destructive ultrasonic pulse velocity method," *Ultrasonics*, vol. 53, no. 5, pp. 962-972, 2013/07/01/ 2013.
- [6] S. Petrusheva, V. Zileska-Pancovska, and D. Car-Pušić, "Implementation of Process-Based and Data-Driven Models for Early Prediction of Construction Time," *Advances in Civil Engineering*, vol. 2019, pp. 1-12, 2019.
- [7] A. Madadi, H. Eskandari-Naddaf, R. Shadnia, and L. Zhang, "Characterization of ferrocement slab panels containing lightweight expanded clay aggregate using digital image correlation technique," *Construction and Building Materials*, vol. 180, pp. 464-476, 2018.
- [8] N.-D. Hoang, "An Artificial Intelligence Method for Asphalt Pavement Pothole Detection Using Least Squares Support Vector Machine and Neural Network with Steerable Filter-Based Feature Extraction," *Advances in Civil Engineering*, vol. 2018, pp. 1-12, 2018.
- [9] T. Dede, M. Kankal, A. R. Vosoughi, M. Grzywiński, and M. Kripka, "Artificial Intelligence Applications in Civil Engineering," *Advances in Civil Engineering*, vol. 2019, pp. 1-3, 2019.
- [10] G. Doğan, M. H. Arslan, and M. Ceylan, "Statistical Feature Extraction Based on an Ann Approach for Estimating the Compressive Strength of Concrete," *Neural Network World*, vol. 25, no. 3, pp. 301-318, 2015.
- [11] G. Dogan, M. H. Arslan, and M. Ceylan, "Concrete compressive strength detection using image processing based new test method," *Measurement*, vol. 109, pp. 137-148, 2017.
- [12] D. Breyse, "Nondestructive evaluation of concrete strength: An historical review and a new perspective by combining NDT methods," *Construction and Building Materials*, vol. 33, pp. 139-163, 2012/08/01/ 2012.